Mon. Not. R. Astron. Soc. **000**, 1–11 (2017) Printed 19 January 2018 (MN LATEX style file v2.2)

The Mira-based distance to the Galactic centre

Wenzer Qin[1]⋆, David M. Nataf[1]†, Nadia L. Zakamska[1],
Peter R. Wood[2], Luca Casagrande[2]

[1]*Center for Astrophysical Sciences and Department of Physics and Astronomy, The Johns Hopkins University, Baltimore, MD 21218,*
[2]*Research School of Astronomy and Astrophysics, Australian National University, Canberra, ACT 2611, Australia*

Accepted ..... Received ..... ; in original form.....

ABSTRACT

Mira variables are useful distance indicators, due to their high luminosities and well-defined period-luminosity relationship. We select 1863 Miras from the SAAO and MACHO surveys to examine their use as distance estimators in the Milky Way. We measure a distance to the Galactic centre of $R_0 = 8.3 \pm 0.2$ kpc, which is in good agreement with other literature values. The uncertainty is dominated by differing interstellar extinction estimates. To improve existing period-luminosity calibrations, we use theoretical models of Miras to determine the dependence of the Mira period-luminosity relation on age, metallicity, and helium abundance. We find that at a fixed period of $\log P = 2.4$, changes in the K_s-band magnitude can be approximated by $\Delta M_{Ks} \approx -0.109(\Delta[\mathrm{Fe/H}]) + 0.033(\Delta \mathrm{t/Gyr}) + 0.021(\Delta \mathrm{Y}/0.01)$, and these coefficients are nearly independent of period. Analogous equations are presented for M_V, M_I, M_J, and M_H. The expected overestimate in the Galactic centre distance from using a relation calibrated to the Large Magellanic Cloud is ∼0.3 kpc, but this prediction cannot be verified given the 0.2 kpc uncertainty in R_0. While the predicted colour-colour diagrams of solar-neighbourhood Miras work very well in the near-infrared, there are offsets from the model predictions in the optical and mid-infrared colours, indicating that these equations should be treated as approximate.

Key words: stars: AGB and post-AGB – stars: variables: general – Galaxy: bulge – Galaxy: centre – galaxies: Magellanic Clouds – infrared: stars.

1 INTRODUCTION

Measurements of Hubble's constant, i.e. the current expansion rate of the universe, are of great interest in modern astrophysics, since its value is a fundamental parameter of Λ-CDM cosmology. Freedman et al. (2012) and Riess et al. (2016) have measured Hubble's constant in the local universe to as low as 2.4% uncertainty. These values are now in tension with other measurements, such as those determined from the cosmic microwave background (Addison et al. 2017; Planck Collaboration et al. 2016). This tension might be due to ground-breaking new physics, so to study the discrepancy it is critical to probe and extend the local distance ladder by independent means.

Mira variables provide a plausible extension to the extragalactic distance scale. They are bright in the infrared for both intermediate-age and old stellar populations, fairly numerous, and have a well-defined period-luminosity relation, and thus one can envisage future catalogues of Mira variables toward great distances produced from *James Webb Space Telescope (JWST)* photometry.

⋆ Email: wqin2@jhu.edu, wenzer.qin@gmail.com
† Email: dnataf1@jhu.edu, david.nataf@gmail.com

Miras are pulsating variable stars that lie in the late evolutionary stages of the asymptotic giant branch (AGB). They are characterized by long pulsation periods of greater than 100 days and high near-infrared and bolometric luminosities. In particular, they have large amplitude variations in infrared and visual wavelengths. Mira variables eject a considerable portion of their mass into surrounding regions, due to their pulsation, and the mass of the resulting circumstellar dust shells is correlated to their periods (Anandarao et al. 1993). Therefore, while all stars experience extinction due the intervening interstellar dust, Miras also experience intrinsic extinction due to circumstellar dust, and this latter phenomenon affects longer period stars the greatest.

AGB variables lie on distinct sequences in diagrams of period versus luminosity, with each sequence corresponding to a different normal mode of pulsation. Mira variables lie on a single sequence, which corresponds to the fundamental mode (Wood & Sebo 1996; Wood 2015). While these sequences are not as tight as those of some other types of variables, most notably Cepheids, they are still quite well-defined. For example, Whitelock et al. (2008) determined a Mira period-luminosity relationship of the form $M_{Ks} = \rho[\log P - 2.38] + \delta$, where the period P is measured in days. The slope, which was calculated using Miras from the Large Mag-

ellanic Cloud (LMC), was determined to be $\rho = -3.51 \pm 0.2$, while the zero-point, which was derived using solar-neighbourhood Miras, was determined to be $\delta = -7.15 \pm 0.07$, assuming an extinction-corrected LMC distance modulus of 18.39 ± 0.05 (van Leeuwen et al. 2007). Thus, the parameters of the Mira period-luminosity relationship can be calculated to better than 6% uncertainty.

If the total extinction of the Miras' light is known, then the period-luminosity relation makes Mira variables useful distance indicators, since

$$\mu = m - M - A \tag{1}$$

where μ is the distance modulus, m is the apparent magnitude, M is the absolute magnitude, and A is the amount of extinction. One goal of this paper is to determine the viability of this technique, since a number of difficulties can arise in making such a distance estimation. First, it is important to select a sample of Mira variables that has sufficient photometric completeness. Nearer stars tend to be brighter, while distant stars are dimmer; therefore, if the sample contains a disproportionate amount of bright or faint stars, this will bias the distance measurements. Secondly, the local Galactic Mira period-luminosity relation determined by Whitelock et al. (2008) has a slope and zero-point based on Miras from the LMC; however, different galaxies vary widely in age and metallicity. The dependence of the period-luminosity relationship on properties such as age and chemical composition has not been probed in great depth, so measurements of distances to other galaxies that rely on an LMC-based period-luminosity relationship may require a correction based on these differences. Therefore, another goal of this paper is to use theoretical models to determine whether such corrections are needed.

We use a complete sample of Miras and improved extinction estimates to measure the distance to the Galactic centre. The Galactic centre provides a useful testbed for using Miras as distance indicators, as its mean distance is measured precisely, and the characteristics of the stellar population in the surrounding Bulge are well-measured. Currently, the best estimate of the distance is $R_0 = 8.2 \pm 0.2$ kpc (Bland-Hawthorn & Gerhard 2016), which was determined by examining distance measurements made using a variety of techniques. However, there is some tension between this value and a recent measurement of 8.9 kpc made using Miras (Catchpole et al. 2016). In this paper, we calculate our own distance estimate, as well as examine issues contributing to the uncertainty in this measurement.

In Section 2, we select a photometrically complete sample of Bulge Miras and state the assumptions we make about the Bulge in fitting the distance to the Galactic centre. In Section 3, we compare the results of measuring distance using different extinction estimates. In Section 4, we examine the dependence of the Mira period-luminosity relationship on age, helium abundance, and metallicity using theoretical models of Mira variables. We conclude our results in Section 5.

2 DATA AND BULGE MODEL ASSUMPTIONS

2.1 Distance measurement method and assumptions

Our intent is to re-examine the distance measurement to the Galactic centre using Mira variables in the Galactic bulge. This is accomplished by plotting the distance modulus of each star in our sample against Galactic longitude, then applying a least-squares fit to the sample and choosing the zero-point of the solution as the Galactic centre (Collinge et al. 2006). To accurately determine R_0, it is important that we choose a photometrically complete sample of Miras. We begin by using 643 Mira variables selected by Catchpole et al. (2016) from two fields observed by the South African Astronomical Observatory (SAAO), 6528 Miras listed by Soszyński et al. (2013) from the Optical Gravitational Lensing Experiment (OGLE), and 1286 Miras from the MACHO survey (Bernhard & Hümmerich 2013; Bernhard et al. 2016; Alcock et al. 1999). We assume these stars are oxygen-rich, since nearly all Bulge Miras are O-rich and contamination by carbon-rich Miras would predominantly occur at very long periods, which we address in section 3.4. In addition, any error introduced by such contamination would not be caused directly by the presence of C-rich Miras, but rather by the difference in contamination rate by C-rich Miras between the Bulge and the LMC (Whitelock et al. 2008).

We cross-match the coordinates of each star with the Wide-field Infrared Survey Explorer, or WISE (Wright et al. 2010), using VizieR with a match radius of 0.5 arcseconds in order to obtain the $W1$ and $W2$ magnitudes. This leaves 635 SAAO Miras, 5821 OGLE Miras, and 1238 MACHO Miras. The distribution of the Miras in Galactic coordinates is shown in Figure 1. We also cross-match all the Miras with the Two Micron All-Sky Survey (2MASS) to obtain the JHK_s photometry for our sample (Skrutskie et al. 2006). Both the WISE and 2MASS magnitudes are calibrated to the Vega scale.

Some of the equations imported for our analysis were derived using SAAO magnitudes. There are no equivalents to these equations that are based on 2MASS measurements, so to make these equations compatible with the 2MASS photometry, we invert the transformations given by Carpenter (2001) and revised at 'www.astro.caltech.edu/~jmc/2mass/v3/transformations/':

$$\begin{aligned}
(K_s)_{2MASS} &= K_{SAAO} - 0.024 + 0.017(J-K)_{SAAO} \\
(J-H)_{2MASS} &= 0.944(J-H)_{SAAO} - 0.048 \\
(J-K_s)_{2MASS} &= 0.944(J-K)_{SAAO} - 0.005 \\
(H-K_s)_{2MASS} &= 0.945(H-K)_{SAAO} - 0.043.
\end{aligned} \tag{2}$$

All values and relationships given from this point forward are in or have been converted to the 2MASS system, unless otherwise specified.

We identify and remove duplicate stars between catalogues if the difference in Galactic longitude and latitude is less than 0.001° and the periods differ by less than 50 days. We find 183 such duplicate stars, which leaves a total of 7511 Miras for analysis. The distribution of Miras in the sky extends over a mean angle of about 5° from the Galactic centre, corresponding to a separation of about 0.7 kpc.

For studying the properties of Miras that do not suffer from significant interstellar extinction, we also obtain 251 solar-neighbourhood Miras and semi-regular variables from Table 1 of Whitelock et al. (2000). These stars were originally observed by *Hipparcos* (ESA 1997), so we obtained the period for each object from the *Hipparcos* data. There are 63 matching objects in the WISE catalogue, which gives $W1$, $W2$, and $W3$ magnitudes. There are also 52 matching objects in the SDSS catalogue (Ahn et al. 2012), which gives $ugriz$ magnitudes on the AB scale.

2.2 Photometry and period data quality

To assess the photometric completeness of each survey, we make the following assumptions. If we wish to sample stars on both the near and far sides of the Bulge, then we require our data to cover distances between 4 and 12 kpc. In addition, the Whitelock et al. (2008) tells

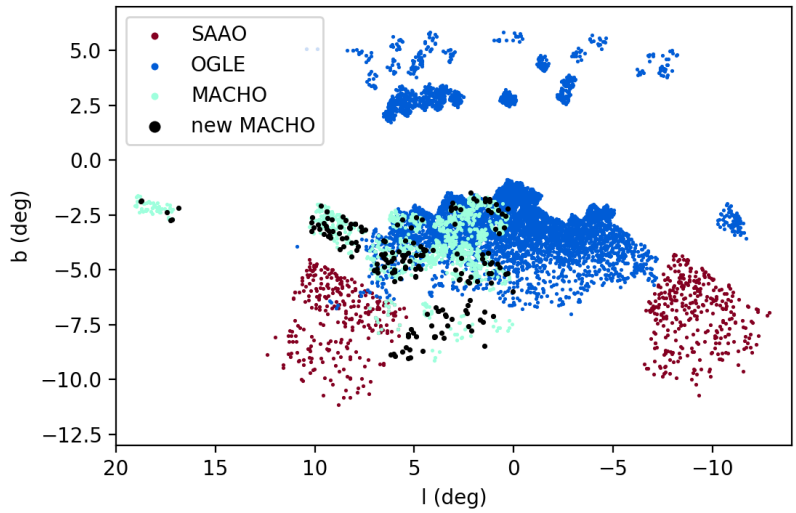

Figure 1. Map in Galactic coordinates of all the Miras used in the study. Each Mira is colour-coded according to the survey that it came from. The newest 192 Miras identified in the MACHO survey are marked in black dots.

us that Miras with periods of $2.1 < \log P < 2.7$ will have a range of absolute K_s-magnitudes between -6.3 and -8.4. Estimating an average extinction of 0.75 and plugging these values in equation 1, we find that to have a Mira sample that is complete on both sides of the bulge, our sample must have apparent K_s-magnitudes at least as bright as 4.6 and at least as faint as 9.8.

We compare distributions of the apparent 2MASS K_s magnitudes for each catalogue in Figure 2. While the SAAO and MACHO Miras show nearly identical K_s magnitude distributions, the OGLE catalogue stars appear shifted towards higher magnitudes, indicating that the survey is comparatively faint. This is not due to incompleteness at the faint end in the SAAO and MACHO samples. As stated previously, to be considered photometrically complete, each sample must cover at least the apparent K_s-magnitudes $4.6 < m_K < 9.8$. Each catalogue is sampled at the faint end and contains stars with $m_K > 10$; however, while both SAAO and MACHO have stars brighter than $m_K = 4.5$, the brightest Mira in the OGLE catalogue is only $m_K = 4.9$. In addition, it has been shown that the MACHO survey is relatively complete in Bulge RR Lyrae stars, which have an average absolute magnitude in the V band of $\overline{M_V} \sim 0$ (Kunder & Chaboyer 2008). According to Table 4 of Kharchenko et al. (2002), Miras are typically brighter, with an average absolute magnitude between $-3.5 < \overline{M_V} < -1$, depending on their periods. This implies that the Miras from the MACHO and SAAO catalogues are well-sampled throughout the Bulge.

If the SAAO and MACHO surveys are as complete as OGLE on the faint end, then the relative shift of the OGLE survey towards higher magnitudes means that the OGLE survey does not contain many of the brighter stars on the near side of the Bulge. This is due to the saturation limit of the OGLE survey at $I \approx 12.5$ mag (Soszyński et al. 2013). Since only a small fraction of overexposed long-period variables are included in the catalogue, the OGLE Miras have low completeness for brighter stars. In addition, since the mean of the I-magnitude distribution for the OGLE Miras is $\bar{I} = 13.77 \pm 1.27$ magnitudes, there is some overlap with the saturation limit. We conclude that a photometrically complete sample of Miras, i.e. a set of Miras that is well sampled throughout the Galactic Bulge, should not contain OGLE stars, which leaves us with 1863 Miras in our sample. Further justification of this is presented in Section 3.4.

In examining the quality flags associated with the 2MASS photometry, we find that less than 3% of the 2MASS measurements were flagged as unreliable or of poor quality. In addition, we find that 77.1% of the WISE measurements are unaffected by artefacts, while 18.5% may be contaminated by scattered light and 4.0% contaminated by diffraction spikes from nearby bright sources, with the remaining 0.4% contaminated by other artefacts. Since the stars affected by 2MASS artefacts constitute only a small fraction of our data and the WISE photometry does not play a central part of the analysis, we have chosen to use the full set of measurements, as the contaminated measurements should not significantly impact our results.

The reliability of the periods determined by SAAO, OGLE, and MACHO is demonstrated by comparing the periods of the duplicate stars discussed previously. If we examine the ratios of the duplicate star periods, we get a mean period ratio of $P_1/P_2 = 1.00 \pm 0.02$, which verifies the reliability of our period data. The *Hipparcos* periods of the solar-neighbourhood Miras that we use have previously been shown to be consistent with other determinations (Whitelock et al. 2000).

2.3 Bulge model

The distance modulus for each star is given by equation (1). The absolute magnitude in the K_s-band is given by the period-luminosity relationship in Whitelock et al. (2008), which we have converted to the 2MASS system:

$$M_{Ks} = -3.50(\log P - 2.38) - 7.257. \quad (3)$$

This relation was transformed by using the first of equations (2) and substituting the $(J-K)_{SAAO}$ colour in that equation with $J - K = -0.39 + 0.71 \log P$, which was derived by Whitelock et al. (2000). The zero-point is 0.1 magnitudes brighter than the best-fitting value that Whitelock et al. (2008) derived from LMC data, as we are using an updated distance modulus to the LMC of

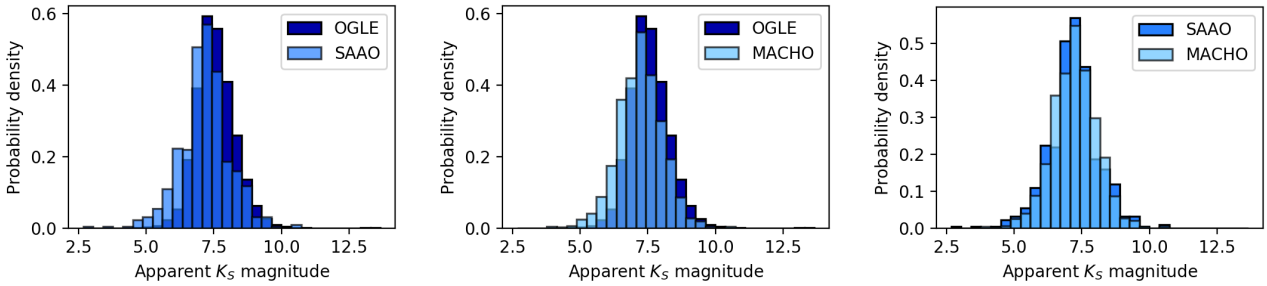

(a) (b) (c)

Figure 2. K_s magnitude distributions of Miras in various catalogues. Each histogram is normalized such that the height represents a probability density. In Figure 2a, there is an offset between the catalogues that indicates the OGLE survey is biased towards fainter stars compared to the SAAO survey. In Figure 2b, the MACHO survey also has a larger left tail, indicating it contains brighter stars than the OGLE survey. In comparison, Figure 2c shows that the distributions for SAAO and MACHO almost completely overlap.

18.49, which is precisely and accurately measured from eight long-period, late-type eclipsing systems composed of cool, giant stars (Pietrzyński et al. 2013). Interestingly, this value is in agreement with that derived by Whitelock et al. (2008) using the *Hipparcos* parallaxes of solar neighbourhood Miras to anchor their distance scale.

For each method of estimating extinction, the distance to the centre of the Galaxy, R_0, is estimated by computing the least-squares fit of distance modulus versus longitude, and then taking the distance at $l = 0°$ as the best fit (Collinge et al. 2006), as shown in Figure 3. Although distance modulus is a logarithmic quantity, the variation in μ is much smaller than the mean value of μ, which allows us to approximate the distance modulus as a linear quantity. The inclination of the modulus-longitude relationship at longer-periods is due to the bar structure of the Bulge. The nearer side of the bar is at positive longitudes, and thus stars at negative longitudes appear fainter on average (Collinge et al. 2006; Catchpole et al. 2016).

The fact that our sample of stars does not cover the Galactic midplane allows us to avoid selection effects caused by the highly filamentary structure of extinction near $|b| = 0$ (Bovy et al. 2016). However, the sample's asymmetric distribution in b does affect our derivation of the distance modulus, since this introduces a dependence on Galactic latitude (Wegg et al. 2015). In fact, Nataf et al. (2016) fit the models of Wegg et al. (2015) to get the following equation for the apparent magnitude of red clump stars in the Bulge

$$I_{RC,0} = 14.3955 - (0.0239 \times l) + (0.0122 \times |b|), \quad (4)$$

which indicates that the expected dependence of distance modulus on latitude is 0.0122 magnitude per degree. The mean absolute latitude of the SAAO and MACHO stars is 4.84°, so this gives an expected offset of 0.06 magnitudes. Assuming $\mu_0 \approx 14.6$, this leads to a distance offset of about 0.23 kpc, which is on the order of other sources of uncertainty. This indicates that the distance moduli we derive require a small geometric correction.

3 EXTINCTION CORRECTIONS

When studying Miras, there are two types of extinction one must take into account. The first is extinction caused by interstellar dust. This is an effect experienced by all types of stars, and the amount of extinction depends on the direction of and distance along the line of sight. The second type of extinction is caused by dust expelled from the Miras, and thus only occurs in the regions near the star. Most extinction maps only measure interstellar extinction; however, there are methods for measuring the total extinction from both interstellar and circumstellar dust and we are careful to make this distinction. Readers interested in the distinction between the circumstellar and interstellar extinction curve of Miras in the infrared are referred to Yuan et al. (2017)

In our study, we compare several different methods of estimating extinction. We use the intrinsic period-colour relations given by Whitelock et al. (2000) and Glass et al. (1995) to predict total extinction. We also use the reddening map described by Schlegel et al. (1998) and recalibrated by Schlafly & Finkbeiner (2011), the reddening map given by Gonzalez et al. (2011, 2012), and the Rayeigh-Jeans colour excess method (Majewski et al. 2011) to measure interstellar extinction only.

The reddening maps of Gonzalez et al. (2012) and Schlafly & Finkbeiner (2011) are "2D" reddening maps, meaning they do not account for the increase in extinction along the line of sight, but rather are mean reddening values for small angular regions on the sky. The error in the extinction estimate from this depth effect is expected to be small, as a typical source from our sample is ~700 pc removed from the Galactic midplane, with none closer than ~200 pc. Since the scale height of dust in the Milky Way is about 125 pc, our sources are far enough from the midplane that the prevalence of dust and, therefore, the dependence of extinction on distance is reduced (Marshall et al. 2006).

3.1 Period-Colour Relations

Whitelock et al. (2000) derive the following relationship between the periods and mean intrinsic colours for local Galactic Miras, which has been transformed to give colours on the 2MASS system:

$$(J - K_s)_0 = -0.37 + 0.67 \log P. \quad (5)$$

Similarly, Glass et al. (1995) give the relationship

$$(J - K_s)_0 = -0.12 + 0.53 \log P. \quad (6)$$

These equations are plotted in Figure 4. By subtracting these relationships from the observed Mira colours, we can obtain the reddening of the Miras' light, or the colour excess in $(J - K_s)$. Reddening and extinction are correlated, since both are caused by dust; however, it is easier to first predict reddening instead of extinction, since an object's intrinsic colour is not affected by its distance. The extinction in K_s can then be derived from the colour excess

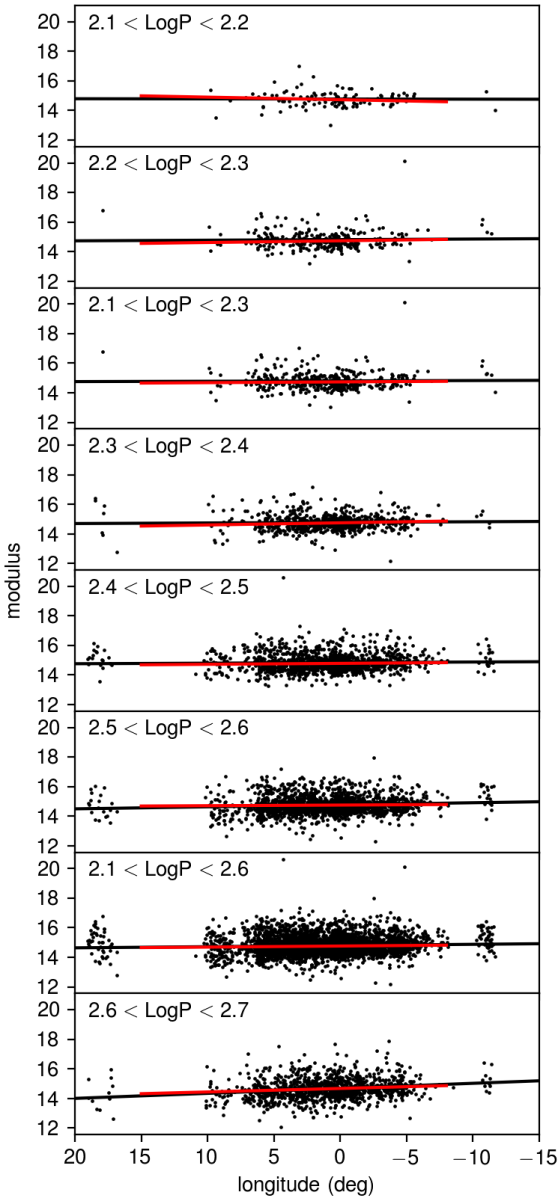

Figure 3. Distance modulus versus longitude for all stars (including OGLE) of different period intervals and $|b| < 4.5°$. The lines represent least-squares fits, with the black line being the fit through all the stars and the red line being the fit through stars with $|l| < 3°$. The zero-points of the fits are given in Table 1.

in $(J - K_s)$ using either the total-to-selective extinction ratio determined by Nishiyama et al. (2009) from Bulge red clump and red giant branch stars:

$$\frac{A_{K_s}}{E(J-K_s)} = 0.495, \tag{7}$$

or that given by Glass (1999):

$$\frac{A_{K_s}}{E(J-K_s)} = 0.53. \tag{8}$$

Combining these equations and extinction coefficients gives four methods of estimating extinction. Since the period-colour relations predict the intrinsic colors of the Miras, they automatically account for both interstellar and circumstellar extinction, making them total extinction maps.

3.2 Dust Reddening Maps

The map described by Schlegel et al. (1998) was recalibrated by Schlafly & Finkbeiner (2011) using stellar spectra from the Sloan Digital Sky Survey (Aihara et al. 2011). The Schlafly & Finkbeiner (2011) map predicts reddening caused by interstellar dust, which is therefore an underestimate of the reddening to our sample, which is often contaminated by circumstellar dust. We use the larger Glass (1999) coefficient to convert the reddening to extinction.

Figure 4 shows the $(J - K_s)$ colours of all Miras dereddened using the Schlafly & Finkbeiner (2011) map, with lines drawn in to represent the period-colour relations given by Whitelock et al. (2000) and Glass et al. (1995). Up to about $\log P \approx 2.6$, the data follows these lines quite well; thus, for Miras of shorter periods, the Schlafly & Finkbeiner (2011) map appears to be in good agreement with the Whitelock et al. (2000) relation converted to 2MASS photometry. Longer period Mira variables have higher mass loss rates, resulting in greater amounts of circumstellar dust, so the discrepancies between the maps at values of $\log P \gtrsim 2.6$ are expected (Whitelock 1990; Anandarao et al. 1993). For stars with $\log P < 2.6$, the Whitelock et al. (2000) reddening estimate is larger than the Schlafly & Finkbeiner (2011) estimate by a median offset of 0.051 magnitudes, indicating the two extinctions maps are consistent with each other up to $\log P \approx 2.6$.

The reddening map described by Gonzalez et al. (2011, 2012) was determined using data from the ESO public survey, *Vista Variables in the Via Lactea*. Similar to the Schlafly & Finkbeiner (2011) extinction map, this map predicts interstellar extinction only, so we paired it with the Glass (1999) ratio. Since the calculator we use only gives values in the region $-10° \leqslant l \leqslant +10.2°$ and $-10° \leqslant b \leqslant +5°$, we could not obtain reddening estimates for several of the stars in our sample. Figure 5a compares the Whitelock et al. (2000) relation and Gonzalez et al. (2012) calculation for the colour excess in $(J - K_s)$. While the data shows the two reddening estimates are generally consistent with one another, there is significant scattering above the line of slope unity. This is, again, due to the fact that the method using the Whitelock et al. (2000) relation estimates both interstellar and circumstellar extinction, while the Gonzalez et al. (2012) map only accounts for interstellar extinction. Figure 5b compares the Schlafly & Finkbeiner (2011) and Gonzalez et al. (2012) extinction estimates, and the plot also shows that the values are generally consistent, since they follow a trend line with a slope of one.

3.3 Rayleigh-Jeans Colour Excess Method

The Rayleigh-Jeans colour excess method described by Majewski et al. (2011) gives the extinction in terms of H and 4.5 μm (or W2) magnitudes and assumes that the intrinsic $(H - [4.5\mu])_0$ colour of the stars being used is 0.08 magnitude:

$$A_{Ks} = 0.918(H - [4.5\mu] - 0.08). \tag{9}$$

However, this method yields a median star distance of 5.22 kpc. The cause of this gross underestimation is most likely that these stars have different mid-infrared colours than what is assumed by equation (9), so we did not include the Rayleigh-Jeans method for further analysis. This issue is revisited in Section 4.

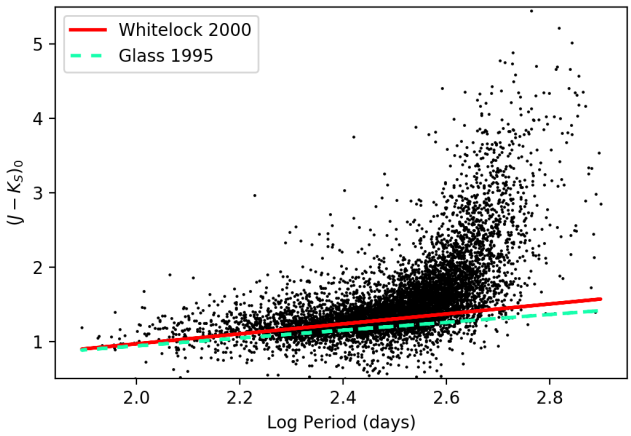

Figure 4. A colour-period diagram of all the Miras, corrected for extinction using the Schlafly & Finkbeiner (2011) reddening map. The lines represent the Whitelock et al. (2000) and Glass et al. (1995) period-colour relations. The lines pass through the densest part of the data until about log $P \approx 2.6$, where circumstellar extinction dominates.

3.4 Comparison of R_0 Estimates

We divide the entire sample of stars into subsets of various period intervals, because of the effect described previously of longer-period stars having greater circumstellar extinction. We then use the method described in Section 2 to calculate R_0 for each dataset. As an example, Table 1 lists various estimates of R_0 using stars in certain intervals of period and Galactic coordinates, with the extinction correction coming from the Whitelock et al. (2000) method, which accounts for both interstellar and circumstellar extinction. Since this initial test of the line fitting includes OGLE objects and used SAAO photometry, the values are in fairly close agreement with the R_0 estimates calculated by Catchpole et al. (2016)—there are small offsets due to our more stringent cross-matching criteria between the 2MASS and WISE catalogues.

To verify that we should not include Mira variables from the OGLE catalogue, we perform the line fittings for each catalogue separately, using the Whitelock et al. (2000) extinction map with the Glass (1999) coefficient. As Table 2 shows, we find that the distances derived from the SAAO and MACHO Miras are both close to 8.2 kpc; however, the OGLE catalogue yields an R_0 value that is larger by about 10%. This is expected given that many of the Miras are brighter than OGLE's saturation limit.

The results of performing the line fittings for each extinction map excluding the OGLE Mira variables are shown in Table 3. In comparison with Table 4, which shows the same line fittings but including OGLE Miras, we see that every method of extinction estimation yields a smaller distance by about 0.7 kpc. This confirms that using the OGLE photometry biases our distance estimate to much higher values. In addition, in Table 3 the distances determined by the period-colour relations are smaller than those determined by the interstellar extinction maps, in part because the period-colour relations apply to individual Mira variables, making them sensitive to even small amounts of circumstellar extinction. The period-colour relations also have the added advantage of not being susceptible to the resolution and depth effects that are inherent in the Schlafly & Finkbeiner (2011) and Gonzalez et al. (2012) reddening maps.

Of the two period-colour relations used, we believe the map given by Whitelock et al. (2000) produces the most reliable distance

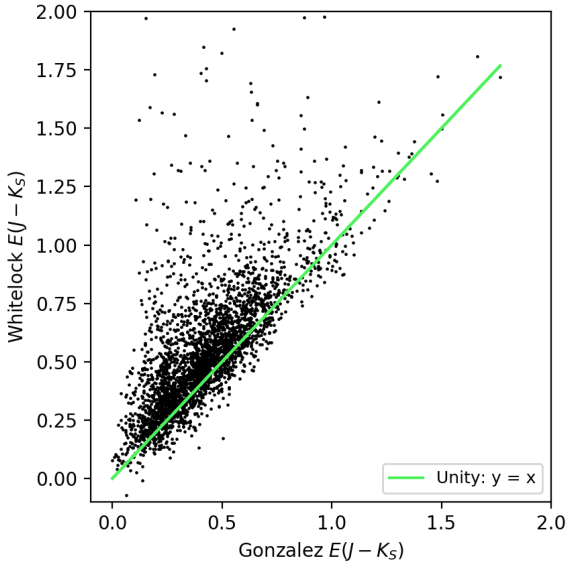

(a)

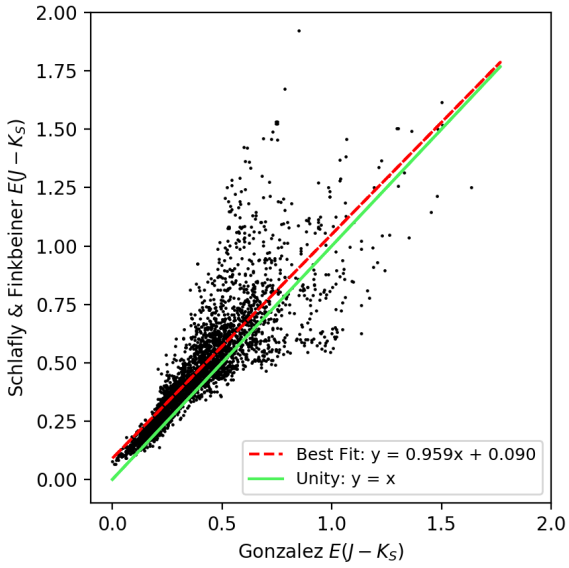

(b)

Figure 5. (5a) Extinction measured according to the method using the Whitelock et al. (2000) relation versus extinction according to the Gonzalez et al. (2012) map, for stars with log $P < 2.5$. The data points above the line $y = x$ are caused by the fact that the Whitelock et al. (2000) method is a total extinction map, while the Gonzalez et al. (2012) map only predicts interstellar extinction. (5b) Extinction measured according to the Schlafly & Finkbeiner (2011) map versus extinction according to the Gonzalez et al. (2012) map, for stars with log $P < 2.5$. The data approximately follows the line of slope unity, indicating that the two extinction estimates are consistent with one another.

estimate. It can be argued that for the purpose of this study, the period-colour relation derived by Glass et al. (1995) is superior to the Whitelock et al. (2000) relation, since the former was determined using Bulge Miras and the latter using solar-neighbourhood Miras. However, the reddening according to the Whitelock et al. (2000) map is more consistent with the Schlafly & Finkbeiner (2011) and

Gonzalez et al. (2012) reddening maps at shorter periods (Figure 4). Therefore, pairing the Whitelock et al. (2000) relation with the Nishiyama et al. (2009) coefficient, which is supported by (Fritz et al. 2011), gives the most reliable extinction estimate.

The conversion from reddening to extinction deserves scrutiny, because there is no conclusively established "best" reddening law for the bulge. Nataf et al. (2016) demonstrated that the reddening law varies significantly from sightline to sightline. For example, their Figure 4 shows a spread of about 40% in the measured values of $A_I/E(V-I)$. The distribution of reddening laws they show includes both the Nishiyama et al. (2009) and Glass (1999) reddening coefficients. There is currently no map of reddening law variations throughout the bulge and we do not have enough colours to calibrate the extinction to reddening ratio for the Miras on a star-by-star basis.

In estimating the distance, we choose to use stars with $\log P < 2.6$, since distances estimated with longer period stars are affected by greater circumstellar extinction, as well as possible contamination by C-rich Miras, as described by Ita & Matsunaga (2011) and Yuan et al. (2017). The effect of C-rich Miras is a point of interest, and merits further investigation, especially in the Bulge.

To summarize, we make the following choices in choosing the best distance estimate for the Galactic Centre:

- Only Miras from the SAAO and MACHO surveys are used, since the OGLE catalogue may be affected by saturation.
- We measure extinction using the Whitelock et al. (2000) period-colour relation, since it measures total extinction and is more consistent with the interstellar dust maps at low periods.
- The extinction estimate is paired with the Nishiyama et al. (2009) extinction to reddening ratio.
- Only stars with $\log P < 2.6$ are used for the line fitting, since longer period stars are affected by greater circumstellar extinction and contamination by C-rich Miras.
- Referring to Table 3, the above choices give a distance of $R_0 = 8.5$ kpc.
- To account for the geometric effect of the Mira latitude distribution, we subtract 0.2 kpc, yielding $R_0 = 8.3$ kpc.

The statistical uncertainties from the different extinction estimates and fitting the distance modulus total to about 0.2 kpc. We exclude the systematic uncertainty associated with using LMC relationships, as this error is addressed in Section 4. Thus, our best and final distance estimate is $R_0 = 8.3 \pm 0.2$ kpc. This is in good agreement with the best estimate from other studies, $R_0 = 8.2 \pm 0.2$ kpc (Bland-Hawthorn & Gerhard 2016).

4 EFFECTS OF AGE AND METALLICITY

In order to investigate the dependence of the Mira K_s–$\log P$ relations on age, metallicity, and helium abundance, we have derived theoretical K_s–$\log P$ relations using the linear, non-adiabatic, radial pulsation code described in Wood & Olivier (2014). This code has been used to identify the pulsation modes associated with the five most prominent period-luminosity sequences exhibited by pulsating AGB stars in the LMC (Wood 2015; Trabucchi et al. 2017). It is assumed that the Mira variables are radial fundamental mode pulsators (Wood 2015). We expect that differential effects on the period caused by changes in mass (age), metallicity and helium abundance are reliable, although the absolute value of the period will have some uncertainty due to the uncertainty in the mixing length parameter of convection.

Table 1. Estimates of R_0 for different intervals of period and Galactic latitude and longitude and using the Whitelock et al. (2000) period-colour relation with the Glass (1999) extinction coefficient. JHK values in the SAAO system were used for the calculations. The sample fitted includes OGLE Miras and excludes the most recent 192 Miras found in the MACHO survey. These values are all in close agreement with the estimates derived by Catchpole et al. (2016).

	All longitudes		**$\lvert l \rvert \leqslant 3°$**	
Period Range	R_0 (kpc)	N	R_0 (kpc)	N
	$\lvert b \rvert < 4.5°$			
$2.1 < \log P < 2.2$	8.857	113	8.664	67
$2.2 < \log P < 2.3$	9.015	310	8.689	198
$2.1 < \log P < 2.3$	8.969	423	8.683	265
$2.3 < \log P < 2.4$	8.879	704	8.744	437
$2.4 < \log P < 2.5$	9.144	1415	8.906	814
$2.5 < \log P < 2.6$	8.820	1785	8.721	1021
$2.1 < \log P < 2.6$	8.949	4327	8.778	2537
$2.6 < \log P < 2.7$	8.368	1104	8.325	622
	$\lvert b \rvert > 4.5°$			
$2.1 < \log P < 2.6$	8.734	1163	9.004	293
$2.6 < \log P < 2.7$	7.985	275	8.444	91
	$\lvert b \rvert > 6.0°$			
$2.1 < \log P < 2.6$	8.233	468	8.397	44
$2.6 < \log P < 2.7$	7.514	89	8.712	19
	SAAO Miras only			
$2.1 < \log P < 2.6$	8.150	512		
$2.6 < \log P < 2.7$	7.389	87		

Table 2. R_0 estimates for each catalogue separately. While the SAAO and MACHO Miras yield similar values, the OGLE catalogue gives a significantly higher distance estimate.

	$2.1 < \log P < 2.6$		**$2.6 < \log P < 2.7$**	
Catalogue	R_0 (kpc)	N	R_0 (kpc)	N
SAAO	8.230	512	7.513	87
OGLE	9.215	4116	8.734	1130
MACHO	8.324	978	7.419	228

The age associated with each K_s–$\log P$ model relation is calculated using the equation

$$\log\left(\frac{M}{M_\odot}\right) = 0.026 + 0.126\,[\mathrm{Fe/H}] - 0.276\log\left(\frac{t}{10}\right) - 0.937(Y - 0.27) \quad (10)$$

Table 3. Estimates of R_0 using different extinction maps and excluding OGLE survey Miras. The sample used includes stars with $|b| < 4.5°$. Names in parentheses indicate the coefficient used to convert between reddening and extinction.

	$2.1 < \log P < 2.6$		**$2.6 < \log P < 2.7$**	
Method	R_0 (kpc)	N	R_0 (kpc)	N
Whitelock (Nishiyama)	8.493	1490	7.622	315
Glass (Nishiyama)	8.318	1490	7.419	315
Whitelock (Glass)	8.442	1490	7.541	315
Glass (Glass)	8.256	1490	7.327	315
Gonzalez	8.901	635	8.684	120
Schlafly	8.578	1490	8.197	315

Table 4. Similar to Table 3, but including OGLE catalogue stars. The R_0 values of Table 3 agree more closely with estimates reported by other studies than the values shown here, possibly because of saturation in the OGLE catalogue.

	2.1 < log P < 2.6		**2.6 < log P < 2.7**	
Method	R_0 (kpc)	N	R_0 (kpc)	N
Whitelock (Nishiyama)	9.220	4327	8.807	1104
Glass (Nishiyama)	9.027	4327	8.572	1104
Whitelock (Glass)	9.120	4327	8.639	1104
Glass (Glass)	8.916	4327	8.392	1104
Gonzalez	9.519	4231	10.308	1086
Schlafly	9.371	4327	10.092	1104

Table 5. Estimated extinction and K_s magnitude errors, using the LMC track (Y = 0.25, [Fe/H] = −0.5, Age = 6 Gyr) as the calibrator. The errors are calculated at the fixed value log P = 2.4. Distance offsets are calculated assuming a distance modulus of 14.6, which is about 8.3 kpc.

Y, [Fe/H], Age	A_{err}	Offset (kpc)	$M_{Ks,err}$	Offset (kpc)
0.25, -0.5, 7	-0.001	0.003	0.036	-0.137
0.29, 0.3, 7	-0.083	0.323	0.032	-0.122
0.37, 0.3, 7	-0.068	0.263	0.197	-0.721
0.25, -0.5, 10	-0.003	0.012	0.137	-0.509
0.29, 0.3, 10	-0.087	0.340	0.132	-0.491
0.37, 0.3, 10	-0.070	0.272	0.294	-1.054
0.27, -0.1, 10 (MW)	-0.045	0.174	0.135	-0.500

from Nataf et al. (2012). Here, [Fe/H] is the metallicity, Y is the helium mass fraction, and t is the age in Gyr. Bolometric corrections are used to obtain the J and K_s magnitudes for each track using the relation

$$M_{Ks} = M_{\mathrm{bol},\odot} - 2.5 \log (L/L_\odot) - BC_{Ks}, \tag{11}$$

where BC stands for bolometric correction. We have used tables of bolometric corrections from Casagrande & VandenBerg (2014) and fixed $M_{\mathrm{bol},\odot} = 4.75$. A similar equation is used for M_J. Using the models, which give P for input values of L, M, Y and [Fe/H], and these relations, we can determine the theoretical period-luminosity and period-colour relations. We fit lines to these relations using a least-squares fit and find that all the tracks are nearly parallel. We then examine how the period-luminosity and period-colour relationships of the theoretical tracks are affected by changes in age, metallicity, or helium abundance. As shown in Figure 6, the period-K_s magnitude relationship depends on all three quantities, while the period-colour relationship depends rather weakly on age and most strongly on metallicity.

From these models, we deduce what the offsets in R_0 would be if we assumed different values for age and metallicity, relative to the R_0 that would be calculated using LMC relations. The extended star formation history in the LMC means that the period-luminosity relation there is defined by multiple masses and ages, as shown by Wood & Sebo (1996) and Wood (2015). However, since the near-infrared colours and magnitudes have an almost linear dependence on age, helium, and metallicity, we conclude that the colour and magnitude at the mean age and metallicity are equal to the mean colour and magnitude of the population as a whole. So, we take the theoretical track at age 6 Gyr, 0.25 helium abundance, and [Fe/H] = −0.5 to represent the LMC (Harris & Zaritsky 2009; Weisz et al. 2013; Choudhury et al. 2016). Using the line fits, we first calculate what the discrepancies in extinction and M_{Ks} would be between the LMC track and other tracks at fixed period (See Table 5). Since the tracks are parallel, these discrepancies remain about the same across different periods. We then convert these errors to distance offsets using $\log(d) = 1 + \mu/5$, where d is in pc and we assume $\mu = 14.6$. Lastly, we interpolate the errors and offsets of the Milky Way relations relative to the LMC, where the track with age 10 Gyr, 0.27 helium, and [Fe/H] = −0.1 is used to approximate the Milky Way Bulge (Nataf 2016; Bensby et al. 2017). We find that the Milky Way track underestimates extinction by −0.045, which would cause our previously calculated R_0 to increase by about 0.2 kpc. On the other hand, the Milky Way track also overestimates the K_s magnitude by 0.135, which would cause the distance estimate to decrease by ∼ 0.5 kpc. Overall, an R_0 value calculated using Milky Way quantities should be smaller than the R_0 calculated assuming LMC relations by ∼ 0.3 kpc.

Regarding the comparison of the Bulge and LMC, the Bulge is definitely ∼ 0.30 dex more metal-rich, on average, than the LMC, though perhaps the difference is really 0.40 dex once the alpha-enhancements are taken into account. We assume that the age is doubled (note that age is a less important factor than metallicity), though we're aware that there is a small controversy as to the exact age distribution for the bulge. For example, Clarkson et al. (2011) rule out a population younger than 5 Gyr, whereas Bensby et al. (2017) estimate that ∼ 20% of bulge stars are younger than 5 Gyr. Given that it is the mean value that matters, this offset will have little impact.

Finally, we determine the coefficients relating changes in J and K_s magnitudes to age, metallicity, and helium abundance. We also include equations for changes in V, I, and H magnitudes, since space-based studies of Miras will make use of these photometric bands (these magnitudes were derived from bolometric corrections in the same way as J and K_s). At a fixed period of log P = 2.4, the changes in these magnitudes can be calculated using

$$\begin{aligned}
\Delta M_V &\approx 6.251\,(\Delta[\mathrm{Fe/H}]) + 0.064\left(\frac{\Delta t}{\mathrm{Gyr}}\right) - 0.044\left(\frac{\Delta Y}{0.01}\right)\\
\Delta M_I &\approx 2.606\,(\Delta[\mathrm{Fe/H}]) + 0.052\left(\frac{\Delta t}{\mathrm{Gyr}}\right) - 0.022\left(\frac{\Delta Y}{0.01}\right)\\
\Delta M_J &\approx 0.085\,(\Delta[\mathrm{Fe/H}]) + 0.035\left(\frac{\Delta t}{\mathrm{Gyr}}\right) + 0.017\left(\frac{\Delta Y}{0.01}\right)\\
\Delta M_H &\approx 0.024\,(\Delta[\mathrm{Fe/H}]) + 0.033\left(\frac{\Delta t}{\mathrm{Gyr}}\right) + 0.020\left(\frac{\Delta Y}{0.01}\right)\\
\Delta M_{Ks} &\approx -0.109\,(\Delta[\mathrm{Fe/H}]) + 0.033\left(\frac{\Delta t}{\mathrm{Gyr}}\right) + 0.021\left(\frac{\Delta Y}{0.01}\right)
\end{aligned} \tag{12}$$

The covariances between changes in age, metallicity, and helium abundance are small. In addition, since the period-luminosity and period-colour relations in the J, H, and K_s bands are parallel for different values of age, metallicity, and helium abundance, the coefficients in equations (12) vary by a negligible amount at different values of log P, so the relations for infrared bands can be used for Miras over a range of log P. However, the V and I equations show a much greater variability with metallicity. For example, at log P = 2.0, the coefficient relating ΔM_V and [Fe/H] is 4.240, while at log P = 2.6 the coefficient is 7.257. Thus, this variable dependence of the V and I equations on metallicity makes it difficult to apply them across a range of periods.

Equations (12) are approximations, since they are based on AGB models and not specifically on Miras. Figure 7 shows colour-colour diagrams for solar-neighbourhood Miras, with lines indicating the colours predicted by the theoretical tracks. The theoretical bolometric corrections used to calculate the various colours are

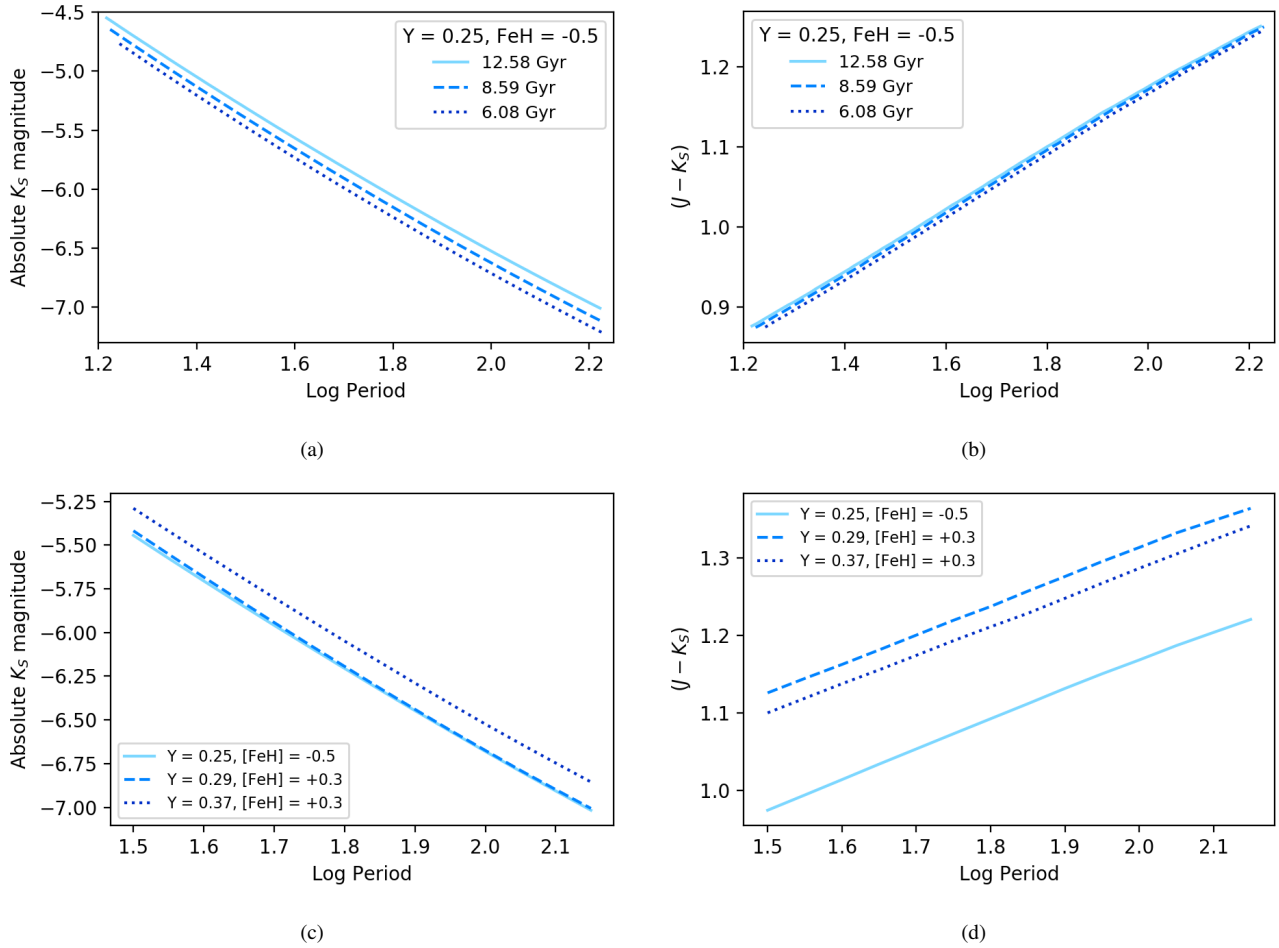

Figure 6. Period-luminosity (K_s) and period-colour relationships obtained from the theoretical AGB models. The left panels show the period-K_s magnitude relationships and the right panels show the period-colour relationships. The top panels show the relationships at fixed metallicity and helium, with varying age. The bottom panels show the relationships at fixed age, with varying helium and metallicity. While the period-K_s magnitude relationship depends on all three quantities, the period-colour relationship has a weak dependence on age and depends most strongly on metallicity.

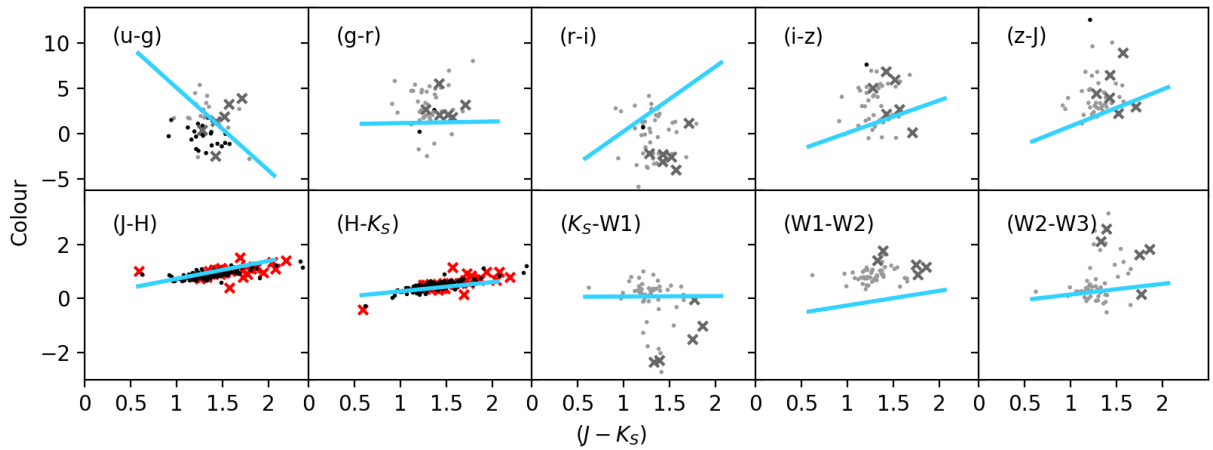

Figure 7. Colour-colour diagrams of solar neighbourhood Miras, where dots represent Miras with log $P < 2.6$ and Xs represent Miras with log $P > 2.6$. Grey dots and Xs indicate measurements that may be affected by saturation and the lines indicate the colours predicted by the AGB models. The y-axis colours are given by the text in each plot, while the x-axis colour is always $(J - K_s)$. The theoretical tracks seem to model the data fairly well in near-infrared colours, but the diagrams showing $ugriz$ and WISE colours indicate that there are still significant discrepancies. This could either be due to the uncertainty in the data due to saturation or the model's failure to reproduce certain colours. Therefore, calculations based on these models should be considered only approximate.

computed in the same way as the J and K_s bolometric corrections described above. In addition, since these stars are within the solar neighbourhood, several of the WISE and SDSS magnitudes suffer from saturation, so sources affected by this are denoted in grey and blue colours (Nikutta et al. 2014 discuss saturation of WISE sources in great detail). While the theoretical colours well match the data in the near-infrared, the tracks do not match nearly as well in the optical or mid-infrared. This discrepancy is either due to the uncertainties in the colours caused by saturation issues, or a deficiency in the model. If it is the latter, then it indicates that the dependencies we get for the period-luminosity relationships only give relative changes, and the coefficients in equations (12) should be considered uncertain.

Lastly, the mean value of $(H-W2)$ for the solar-neighbourhood Miras is 1.29 magnitudes. Referring back to Section 3.3, this is considerably higher than the 0.08 magnitude mean assumed by the Rayleigh-Jeans colour excess method of calculating extinction. Therefore, the colours of the Miras we use give overly large extinction estimates, which explains why the median star distance was only 5.22 kpc, justifying our decision to not include the Rayleigh-Jeans method in our analysis.

5 CONCLUSION

In this study, we examine the validity of making distance measurements using Mira variables by using them to measure the distance to the Galactic centre, as well as probing the dependence of the Mira period-luminosity relation on a galaxy's age and composition. In selecting an ideal sample of Bulge Miras for fitting the distance to the Galactic centre, we find that the OGLE catalogue (Soszyński et al. 2013) has low completeness for brighter stars (i.e., stars on the near side of the Bulge), making it unsuitable to use for our distance study. In comparing several methods of estimating extinction, we find that colour-based techniques for calculating extinction towards Miras work better than Galactic dust maps, since the former method allows us to correct the apparent magnitude for both interstellar and circumstellar extinction. After applying such a method, choosing stars with periods $\log P < 2.6$, and making a geometric correction, we determine that our best estimate for the distance to the Galactic centre is $R_0 = 8.3 \pm 0.2$ kpc, which is in good agreement with measurements of R_0 based on other methods in the literature (Bland-Hawthorn & Gerhard 2016).

We use theoretical tracks and bolometric corrections to model Mira period-luminosity and period-colour relations and study their dependence on age and chemical composition. In comparing the colors predicted by these models to the colors of solar-neighborhood Miras, we find discrepancies in the optical and near-infrared photometric bands, which is either due to saturation or deficiencies in the models. This suggests that the relationships we derive should only be used as approximations.

However, assuming that these models are valid for Galactic Miras, we find that there is a non-negligible dependence of the relations on metallicity and helium, with a smaller effect from stellar age. Since the Milky Way Bulge is about twice as old and twice as metal-rich as the LMC, using relations based on the LMC should cause an overestimate of R_0 on the order of ~ 0.3 kpc. Thus, as we strive to use Mira variables to make increasingly precise distance estimates, both within and outside of the Galaxy, accurately determining the variation of the period-luminosity relations from galaxy to galaxy will become more important.

ACKNOWLEDGMENTS

WQ was supported by NASA's Maryland Space Grant Consortium. DMN was supported by the Allan C. and Dorothy H. Davis Fellowship. NLZ was supported by the Johns Hopkins University Catalyst Award. LC gratefully acknowledges support from the Australian Research Council (grants DP150100250, FT160100402). We would like to thank an anonymous referee whose comments have been valuable in improving this work. We made use of the VizieR and SIMBAD databases of the CDS in preparing this paper. This paper uses observations made at the South African Astronomical Observatory (SAAO). The OGLE project has received funding from the National Science Centre, Poland, grant MAESTRO 2014/14/A/S3T9/00121 to AU. This paper utilizes public domain data obtained by the MACHO Project, jointly funded by the US Department of Energy through the University of California, Lawrence Livermore National Laboratory under contract No. W-7405-Eng-48, by the National Science Foundation through the Center for Particle Astrophysics of the University of California under cooperative agreement AST-8809616, and by the Mount Stromlo and Siding Spring Observatory, part of the Australian National University. This publication makes use of data products from the Two Micron All Sky Survey, which is a joint project of the University of Massachusetts and the Infrared Processing and Analysis Center/California Institute of Technology, funded by the National Aeronautics and Space Administration and the National Science Foundation. This publication makes use of data products from the Wide-field Infrared Survey Explorer, which is a joint project of the University of California, Los Angeles, and the Jet Propulsion Laboratory/California Institute of Technology, funded by the National Aeronautics and Space Administration.

REFERENCES

Addison G. E., Watts D. J., Bennett C. L., Halpern M., Hinshaw G., Weiland J. L., 2017, preprint (arXiv:1707.06547)
Ahn C. P. et al., 2012, ApJS, 203, 21
Aihara H. et al., 2011, ApJS, 193, 29
Alcock C. et al., 1999, PASP, 111, 1539
Anandarao B. G., Pottasch S. R., Vaidya D. B., 1993, A&A, 273, 570
Bensby T. et al., 2017, A&A, 605, A89
Bernhard A., Hümmerich S., 2013, Open European Journal on Variable Stars, 159, 1
Bernhard K., Uttenthaler S., Hümmerich S., 2016, ArXiv e-prints
Bland-Hawthorn J., Gerhard O., 2016, ARA&A, 54, 529
Bovy J., Rix H. W., Green G. M., Schlafly E. F., Finkbeiner D. P., 2016, ApJ, 818, 130
Carpenter J. M., 2001, AJ, 121, 2851
Casagrande L., VandenBerg D. A., 2014, MNRAS, 444, 392
Catchpole R. M., Whitelock P. A., Feast M. W., Hughes S. M. G., Irwin M., Alard C., 2016, MNRAS, 455, 2216
Choudhury S., Subramaniam A., Cole A. A., 2016, MNRAS, 455, 1855
Clarkson W. I. et al., 2011, ApJ, 735, 37
Collinge M. J., Sumi T., Fabrycky D., 2006, ApJ, 651, 197
ESA, ed., 1997, The HIPPARCOS and TYCHO catalogues. Astrometric and photometric star catalogues derived from the ESA HIPPARCOS Space Astrometry Mission, ESA Special Publication, Vol. 1200
Freedman W. L., Madore B. F., Scowcroft V., Burns C., Monson A., Persson S. E., Seibert M., Rigby J., 2012, ApJ, 758, 24

Fritz T. K. et al., 2011, ApJ, 737, 73
Glass I. S., 1999, Handbook of Infrared Astronomy. Cambridge University Press
Glass I. S., Whitelock P. A., Catchpole R. M., Feast M. W., 1995, MNRAS, 273, 383
Gonzalez O. A., Rejkuba M., Zoccali M., Valenti E., Minniti D., 2011, A&A, 534, A3
Gonzalez O. A., Rejkuba M., Zoccali M., Valenti E., Minniti D., Schultheis M., Tobar R., Chen B., 2012, A&A, 543, A13
Harris J., Zaritsky D., 2009, AJ, 138, 1243
Ita Y., Matsunaga N., 2011, MNRAS, 412, 2345
Kharchenko N., Kilpio E., Malkov O., Schilbach E., 2002, A&A, 384, 925
Kunder A., Chaboyer B., 2008, AJ, 136, 2441
Majewski S. R., Zasowski G., Nidever D. L., 2011, ApJ, 739, 25
Marshall D. J., Robin A. C., Reylé C., Schultheis M., Picaud S., 2006, A&A, 453, 635
Nataf D. M., 2016, PASA, 33, e023
Nataf D. M., Gould A., Pinsonneault M. H., 2012, Acta. Astronom., 62, 33
Nataf D. M. et al., 2016, MNRAS, 456, 2692
Nikutta R., Hunt-Walker N., Nenkova M., Ivezić Ž., Elitzur M., 2014, MNRAS, 442, 3361
Nishiyama S., Tamura M., Hatano H., Kato D., Tanabé T., Sugitani K., Nagata T., 2009, ApJ, 696, 1407
Pietrzyński G. et al., 2013, Nature, 495, 76
Planck Collaboration et al., 2016, A&A, 594, A13
Riess A. G. et al., 2016, ApJ, 826, 56
Schlafly E. F., Finkbeiner D. P., 2011, ApJ, 737, 103
Schlegel D. J., Finkbeiner D. P., Davis M., 1998, ApJ, 500, 525
Skrutskie M. F. et al., 2006, AJ, 131, 1163
Soszyński I. et al., 2013, Acta. Astronom., 63, 21
Trabucchi M., Wood P. R., Montalbán J., Marigo P., Pastorelli G., Girardi L., 2017, ApJ, 847, 139
van Leeuwen F., Feast M. W., Whitelock P. A., Laney C. D., 2007, MNRAS, 379, 723
Wegg C., Gerhard O., Portail M., 2015, MNRAS, 450, 4050
Weisz D. R., Dolphin A. E., Skillman E. D., Holtzman J., Dalcanton J. J., Cole A. A., Neary K., 2013, MNRAS, 431, 364
Whitelock P., Marang F., Feast M., 2000, MNRAS, 319, 728
Whitelock P. A., 1990, in C. Cacciari, G. Clementini, eds, Confrontation Between Stellar Pulsation and Evolution. Astronomical Society of the Pacific Conference Series, Vol. 11, pp. 365–378
Whitelock P. A., Feast M. W., Van Leeuwen F., 2008, MNRAS, 386, 313
Wood P. R., 2015, MNRAS, 448, 3829
Wood P. R., Olivier E. A., 2014, MNRAS, 440, 2576
Wood P. R., Sebo K. M., 1996, MNRAS, 282, 958
Wright E. L. et al., 2010, AJ, 140, 1868-1881
Yuan W., Macri L. M., He S., Huang J. Z., Kanbur S. M., Ngeow C. C., 2017, AJ, 154, 149